



**HAL**  
open science

## Refining uptake and depuration constants for fluoroalkyl chemicals in *Chironomus riparius* larvae on the basis of experimental results and modelling

Delphine Bertin, Benoît J.D. Ferrari, Pierre Labadie, Alexandre Sapin, Débora da Silva Avelar, Rémy Beaudouin, Alexandre R.R. Pery, Jeanne Garric, Hélène Budzinski, Marc Babut

### ► To cite this version:

Delphine Bertin, Benoît J.D. Ferrari, Pierre Labadie, Alexandre Sapin, Débora da Silva Avelar, et al.. Refining uptake and depuration constants for fluoroalkyl chemicals in *Chironomus riparius* larvae on the basis of experimental results and modelling. *Ecotoxicology and Environmental Safety*, 2018, 149, pp.284-290. 10.1016/j.ecoenv.2017.12.011 . hal-01666918

**HAL Id: hal-01666918**

**<https://hal.science/hal-01666918>**

Submitted on 16 May 2020

**HAL** is a multi-disciplinary open access archive for the deposit and dissemination of scientific research documents, whether they are published or not. The documents may come from teaching and research institutions in France or abroad, or from public or private research centers.

L'archive ouverte pluridisciplinaire **HAL**, est destinée au dépôt et à la diffusion de documents scientifiques de niveau recherche, publiés ou non, émanant des établissements d'enseignement et de recherche français ou étrangers, des laboratoires publics ou privés.



Distributed under a Creative Commons Attribution - ShareAlike 4.0 International License

## **Refining uptake and depuration constants for fluoroalkyl chemicals in *Chironomus riparius* larvae on the basis of experimental results and modelling**

Delphine Bertin<sup>a</sup>, Benoît J. D. Ferrari<sup>a,b</sup>, Pierre Labadie<sup>c</sup>, Alexandre Sapin<sup>a</sup>, Débora Da Silva Avelar<sup>a</sup>, Rémy Beaudouin<sup>d</sup>, Alexandre Péry<sup>e,f</sup>, Jeanne Garric<sup>a</sup>, Hélène Budzinski<sup>c</sup>, Marc Babut<sup>a\*</sup>

<sup>a</sup> IRSTEA, UR MALY, 5 rue de la Doua, BP 32108, F- 69616 Villeurbanne, France;

<sup>b</sup> Swiss Centre for Applied Ecotoxicology Eawag-EPFL (CentreEcotox), EPFL-ENAC-II-GE, Station 2, CH-1015 Lausanne, Switzerland;

<sup>c</sup> CNRS, UMR 5805 EPOC (LPTC Research group), Université de Bordeaux, 351 Cours de la Libération, F-33405 TALENCE, France;

<sup>d</sup> Unité Modèles pour l'Ecotoxicologie et la Toxicologie (METO), Institut National de l'Environnement Industriel et des Risques (INERIS), BP2, F-60550 Verneuil en Halatte, France

<sup>e</sup> AgroParisTech, UMR 1402 INRA-AgroParisTech EcoSys, F-78850 THIVERVAL-GRIGNON, France

<sup>f</sup> INRA, UMR 1402 INRA-AgroParisTech EcoSys, F-78850 THIVERVAL-GRIGNON, France

### Present addresses

- Delphine Bertin, UMR 5023 LEHNA (E3S Research group), Université Claude-Bernard Lyon 1, 6 rue Raphaël Dubois, 69622 Villeurbanne, Cedex, France  
[delphine.bertin@univ-lyon1.fr](mailto:delphine.bertin@univ-lyon1.fr)
- [Débora Da Silva Avelar: dhezinha@gmail.com](mailto:dhezinha@gmail.com)
- Alexandre Sapin - Rovaltain Research Company BP 10 313, F-26958 Valence cedex 9, France; [asapin@rovaltainresearch.com](mailto:asapin@rovaltainresearch.com)

## Role of the funding source

The laboratory experiments and analyses were mainly funded by the Rhone-Mediterranean and Corsica Water Agency and the Rhône-Alps Region within the Rhône ecological restoration plan. Additional grants were obtained from the Aquitaine Region and the European Union (CPER A2E project), and the French National Research Agency (ANR) as part of the Investments for the Future Program, within the Cluster of Excellence COTE (ANR-10-LABX-45). None of these supports were involved in the study design, nor in data processing, report writing and article submission.

## 1 **Highlights**

- 2 • Chironomids were exposed to sediment contaminated by fluoro-alkyl substances.
- 3 • For all compounds, nearly complete elimination from tissues was achieved in 42 h.
- 4 • Modeling shows that PFTrDA uptake is concentration-dependent.

## 5 **Abstract**

6 The aims of this study were to determine depuration rates for a range of per- and  
7 polyfluoroalkyl substances (PFASs) using *Chironomus riparius*, and to test a concentration-  
8 dependency hypothesis for the long-chain perfluorotridecanoic acid (PFTrDA) for this  
9 species. Midge larvae were exposed to field sediments collected downstream of a  
10 fluorotelomer plant, and to the same sediment spiked with PFTrDA. Elimination kinetics  
11 results indicated complete elimination of all PFASs by chironomids after 42 h. These data  
12 were used to develop two PFTrDA bioaccumulation models accounting for chironomid  
13 growth and for compound concentration dependency or not. There was much better agreement  
14 between observed and simulated data under the concentration-dependency hypothesis than  
15 under the alternative one (passive diffusion). The PFTrDA uptake rate derived from the  
16 concentration-dependency model equaled  $0.013 \pm 0.008 g_{oc} \cdot g_{ww}^{-1} \cdot h^{-1}$ , and the depuration rate  
17  $0.032 \pm 0.009 h^{-1}$ .

## 18 **Keywords**

19 Per- and polyfluoroalkyl substances; perfluorotridecanoic acid; *Chironomus riparius*;  
20 bioaccumulation; uptake rate; concentration-dependency

## 21 **1. Introduction**

22 Perfluoroalkyl and polyfluoroalkyl substances (PFASs) are compounds of emerging interest;  
23 their numerous uses and specific properties induce their global distribution in the environment  
24 (Houde et al., 2011; Houde et al., 2006; Prevedouros et al., 2006). The physicochemical

25 properties of PFASs differ substantially from those of other persistent organic pollutants  
26 (POPs). While the perfluoroalkyl moiety is hydrophobic and lipophobic (Bhatarai and  
27 Gramatica, 2011), the functional group increases the solubility in water, and per- and  
28 polyfluoroalkyl acids are thus amphiphilic. These complex properties make it difficult to  
29 predict their bioaccumulation, even though it seems that the bioaccumulation of longer-chain  
30 PFASs is partly driven by their increasing lipophilic character (Greaves et al., 2013). Several  
31 studies have shown the presence of PFASs in sediment (Ahrens et al., 2009; Bao et al., 2009;  
32 Bao et al., 2010; Higgins et al., 2005; Labadie and Chevreuil, 2011; Myers et al., 2012; Zushi  
33 et al., 2010), whereas other studies have suggested the importance of sediment as a PFAS  
34 source for biota (e.g., Martin et al., 2004). However, PFAS transfer from sediment to biota is  
35 poorly understood. Only a few experimental studies have provided evidence of  
36 bioaccumulation from sediment by benthic invertebrates, namely in the oligochaete worm,  
37 *Lumbriculus variegatus* (Higgins et al., 2007; Lasier et al., 2011; Prosser et al., 2016), in  
38 insect *Chironomus riparius* (Bertin et al., 2014) and *Hexagenia* spp. larvae (Prosser et al.,  
39 2016), and in an amphipod, *Gammarus* spp. (Bertin et al., 2016). Two contamination routes  
40 were identified for *C. riparius*: food was the main route of exposure for perfluorinated  
41 carboxylic acids (PFCAs) with a fluorinated chain from C<sub>11</sub> to C<sub>14</sub>, and perfluorooctane  
42 sulfonamide (FOSA). For perfluoroundecanoic acid (PFUnDA), perfluorooctane sulfonate  
43 (PFOS), and 6:2 fluorotelomer sulfonic acid (6:2 FTSA), which are present in pore water  
44 (PW) and sediment, both uptake from water (i.e. respiration) and from food were involved.  
45 Accumulated concentrations in this species fit an exponential curve which could be supported  
46 by two models: (i) a classical partition model (Higgins et al., 2007), which assumes that the  
47 PFASs concentrations in organisms and sediment at steady state are proportional; and (ii) a  
48 concentration-dependency model (Liu et al., 2011), which hypothesizes that the uptake  
49 kinetics involves active transport through binding to specific sorption sites, such that these

50 sites may become saturated at high exposure concentrations. To gain a more accurate  
51 understanding of the processes underpinning the PFAS uptake mechanisms for chironomids,  
52 and to refine the uptake and depuration constants, the models proposed must be tested to  
53 determine which is the most suitable.

54 The aims of the present study were therefore (i) to describe PFAS elimination kinetics for  
55 chironomids, and (ii) to test the concentration dependency of the PFAS bioaccumulation for a  
56 model compound, the perfluorotridecanoic acid (PFTTrDA). A combined accumulation and  
57 depuration experiment involving field sediment was implemented to address the first  
58 objective. For the second one, we conducted combined accumulation and depuration  
59 experiments at different concentrations and applied a bioaccumulation model adapted to these  
60 compounds and species that could account for realistic kinetics constants.

## 61 **2. Bioaccumulation modeling: theoretical background**

62 Assuming that PFAS uptake and elimination depend on the organisms' surface, the dynamics  
63 of the PFAS load in the organism are defined as follows:

$$64 \quad \frac{d(Q_{org})}{dt} = S_{org} \cdot k_u \cdot C_{sed-oc} - S_{org} \cdot k_e \cdot C_{org} \quad \text{Eq. (1)}$$

65 where  $Q_{org}$  corresponds to the quantity of PFASs in and/or on the organism,  $S_{org}$  the  
66 chironomids surface,  $k_u$  ( $\text{g} \cdot \text{g}_{\text{ww}} \cdot \text{mm}^{-2} \cdot \text{d}^{-1}$ ) and  $k_e$  ( $\text{mm}^{-2} \cdot \text{d}^{-1}$ ) the uptake and elimination  
67 constants, respectively.  $C_{sed-oc}$  ( $\text{ng} \cdot \text{g}_{\text{oc}}^{-1} \cdot \text{dw}$ ) and  $C_{org}$  ( $\text{ng} \cdot \text{g}_{\text{ww}}^{-1}$ ) indicate the PFAS  
68 concentrations in sediment adjusted to the  $f_{oc}$ , and in the organisms, respectively. As a  
69 consequence of growth during the test (Péry et al., 2002), the tissue concentration dynamics is  
70 described by Eq. 2 (details in SI):

$$71 \quad \frac{d(C_{org})}{dt} = \left( \frac{1}{L} \cdot k_u \cdot C_{sed-oc} - \frac{1}{L} \cdot k_e \cdot C_{org} \right) - C_{org} \times \frac{d(V)}{dt} \times \frac{1}{V} \quad \text{Eq. (2)}$$

72 Where  $C_{org}$  is the internal concentration,  $L$  is the chironomids length (cm), and  $V$  is the

73 chironomid volume (cm<sup>3</sup>). Note that  $k_u$  and  $k_e$  in Eq. (2) are expressed in different units than  
74 in Eq. (1), namely  $g_{oc} \cdot g_{ww} \cdot h^{-1}$  for  $k_u$  and  $h^{-1}$  for  $k_e$ .

75 PFAS uptake may or may not be concentration-dependent, i.e. this uptake could follow either  
76 first order kinetics or kinetics with saturation. In case of concentration-dependency, the  
77 accumulation can be viewed as an adsorption-like process, in which the chemical adsorb at  
78 binding sites, i.e. specific components of the organs where PFASs accumulate (Liu et al.,  
79 2011). The binding site saturation process progressively slows down the uptake, and the  
80 steady state is reached at a lower concentration than in the case of a first order kinetics. Both  
81 the concentration in the exposure media and the number of sites remaining free control the  
82 uptake rate. The  $S$  term was introduced in order to model these two cases:

$$83 \quad S = \frac{1}{\left(1 + \frac{C_{org}}{C_{50}}\right)} \quad \text{Eq. (3)}$$

84 with  $C_{50}$  representing the half-saturation concentration, i.e. the internal concentration at which  
85 the uptake is one-half of its maximum rate. When  $C_{org}$  is low,  $S$  is close to 1, and the  
86 dynamics follow Eq. 2; conversely, when  $C_{org}$  increases and site binding occurs,  $S$  decreases  
87 and tends to 0, meaning that the uptake is lower or stopped. The final equation is:

$$88 \quad \frac{d(C_{org})}{dt} = \left(\frac{1}{L} \cdot k_u \cdot C_{sed-oc} \cdot S - \frac{1}{L} \cdot k_e \cdot C_{org}\right) - C_{org} \times \frac{d(V)}{dt} \times \frac{1}{V} \quad \text{Eq. (4)}$$

89 A half-life ( $T_{1/2}$ ) can be derived from the model as the time necessary for a 50% decrease in  
90 the accumulated concentration.

### 91 3. Materials and Methods

#### 92 3.1. Chemicals

93 Standard PFAS solutions (PFC-MXA and PFS-MXA) were obtained from Wellington  
94 Laboratories (via BCP Instruments, Irigny, France): PFC-MXA contained perfluoro-n-

95 butanoic acid (PFBA), perfluoro-n-pentanoic acid (PFPA), perfluoro-n-hexanoic acid  
96 (PFHxA), perfluoro-n-heptanoic acid (PFHpA), perfluoro-n-octanoic acid (PFOA), perfluoro-  
97 n-nonanoic acid (PFNA), perfluoro-n-decanoic acid (PFDA), perfluoro-n-undecanoic acid  
98 (PFUnDA), perfluoro-n-dodecanoic acid (PFDoDA), perfluoro-n-tridecanoic acid (PFTrDA),  
99 and perfluoro-n-tetradecanoic acid (PFTeDA), each at 2 ng.μL<sup>-1</sup> in methanol (MeOH). PFS-  
100 MXA contained perfluoro-1-butanesulfonate (PFBS) potassium salt, perfluoro-1-  
101 hexanesulfonate PFHxS) sodium salt, perfluoro-1-heptanesulfonate (PFHpS) sodium salt, n-  
102 perfluoro-1-octanesulfonate (PFOS) sodium salt and perfluoro-1-decanesulfonate (PFDS)  
103 sodium salt, N-Ethyl perfluorooctane sulfonamide (EtFOSA), N-Methyl perfluorooctane  
104 sulfonamide (MeFOSA), perfluorooctane sulfonamide (FOSA), N-Ethyl perfluorooctane  
105 sulfonamidoacetic acid (EtFOSAA), N-Methyl perfluorooctane sulfonamidoacetic acid  
106 (MeFOSAA), and 6:2 Fluorotelomer sulfonic acid (6:2 FTSA), each at 2 ng.μL<sup>-1</sup> in MeOH.  
107 A working solution containing all analytes, each at approximately 0.05 ng.μL<sup>-1</sup>, was prepared  
108 in MeOH and stored at -18°C. <sup>13</sup>C-labelled perfluorodecanoic acid (PFDA), PFOS, and  
109 perfluorooctane sulfonamide (FOSA), each at 50 ng.μL<sup>-1</sup> in MeOH, were supplied by  
110 Wellington Laboratories and used as internal standards (ISs). A working solution was  
111 prepared in MeOH, each containing IS at 0.1 ng.μL<sup>-1</sup> (Table S1 in supplementary  
112 information).

113 LC/MS-grade MeOH and acetonitrile (ACN) were purchased from J.T. Baker via Interchim  
114 (Montluçon, France). Sodium acetate buffer (99%, ACS Reagent), ammonium hydroxide (28–  
115 30% in water), 0.2-μm nylon centrifuge tube filters, and ENVI-Carb cartridges (6 cc, 250 mg)  
116 were obtained from Sigma-Aldrich (St Quentin Fallavier, France), whereas Strata XAW (6  
117 ml, 200 mg) were purchased from Phenomenex (Le Pecq, France). Nitrogen (99%) was  
118 supplied by Air Liquide (Paris, France). Ultra-pure water was obtained using an Elix 10  
119 purification system fitted with an EDS pack (Millipore, Guyancourt, France).

## 120 3.2. Testing strategy

121 Two experiments were conducted with *C. riparius*: an accumulation test with field and field-  
122 spiked sediment, and an elimination test with field and field-spiked sediment (Figure S1 in  
123 SI). The decision to spike field sediment was made for testing the concentration-dependency  
124 hypothesis; spiking involved PFTrDA, the main PFAS among those detected in the field  
125 sediment used in the present study (Munoz et al., 2015). The elimination experiment was  
126 implemented in order to improve the accumulation kinetics modelling when concentration-  
127 dependency occurs (Bertin et al., 2014).

### 128 3.2.1. Field sediment

129 The study was conducted using sediment collected at Beurre Island (characteristics in SI).  
130 This site is a fluvial annex of the Rhone River (eastern central France,  
131 N45°28'17.0"E4°46'43.4") located downstream of a fluoropolymer manufacturing plant.  
132 Since 1902, this industrial site has been used to produce hydrofluoric acid and a wide array of  
133 fluorine-based organics. Three PFAS production periods can be defined at this site: (i)  
134 polytetrafluoroethylene (PTFE) production from 1960 to 1987, (ii) fluorinated copolymers  
135 synthesis from 1981 to 1996, and (iii) polyvinylfluoridene (PVDF) production from  $\approx$  1981  
136 onwards (Dauchy et al., 2012). Two campaigns were conducted in 2013 (March and  
137 November): 50 L of surface sediments ( $\approx$  5 cm deep) were collected from the river bed with a  
138 Van-Veen grab, kept on ice, and brought to the laboratory, where they were sieved at 2 mm,  
139 pooled in a polypropylene (PP) jar, and stored at 4°C.

### 140 3.2.2. Sediment spiking

141 In order to test the concentration-dependency hypothesis, field sediments were spiked with  
142 PFTrDA, on the basis of the field sediment contamination pattern (Munoz et al., 2015), and  
143 on the chironomids accumulation capacity (Bertin et al., 2014). The loss of ignition (LOI)

144 values of these sediments laid between 5.2 % and 5.4 %, corresponding to organic carbon  
145 fractions ( $f_{oc}$ ) of 0.02 (conversion factor of 2.4 based on Craft et al.,1991). The spiking  
146 solution was prepared with a stock solution purchased from Wellington Laboratories (via  
147 BCP Instruments, Irigny, France). For each concentration, a PFTrDA solution ( $0.1 \text{ g.L}^{-1}$  in  
148 MeOH) was added to 1.2 L of sediment and 0.4 L of clean water. The bottles were gently  
149 shaken for 6 h; the sediment was then allowed to settle for 48 h and the overlying water (OW)  
150 cautiously siphoned off. The sediment was then homogenised and subsequently reintroduced  
151 in aquaria for chironomid exposure. In the first experiment, PFTrDA was added at twice (C1)  
152 its initial concentration in the field sediment ( $1.64 \pm 0.03 \text{ ng.g}^{-1} \text{ dw}$ ). The accumulation phase  
153 was reduced to 2 days, in order to increase the duration of the depuration period and get more  
154 samples for this phase. For a second experiment PFTrDA was added at approximately five  
155 times (C2) the initial field sediment concentration ( $1.67 \pm 0.48 \text{ ng.g}^{-1} \text{ dw}$ ) and ten times (C3)  
156 the field sediment concentration ( $1.67 \pm 0.48 \text{ ng.g}^{-1} \text{ dw}$ ). Note that two different batches of  
157 field sediments were used for these experiments, displaying similar PFTrDA concentrations at  
158  $1.64 \pm 0.03 \text{ ng.g}^{-1} \text{ dw}$  and  $1.67 \pm 0.48 \text{ ng.g}^{-1} \text{ dw}$  (Table S2). Sediment depth after transfer in  
159 the aquaria was approximately 5 cm.

### 160 3.2.3. *Chironomus riparius* accumulation and depuration tests

161 Chironomids were obtained from our laboratory cultures maintained according to standard  
162 methods (OECD, 2004; AFNOR, 2010). Experiments were conducted in the same laboratory  
163 conditions as previously described by Bertin et al. (2014). Briefly, *C. riparius* fourth instar  
164 (L4) larvae (7-day-old larvae post-hatching) were exposed to field sediment covered with  
165 OW, i.e., a mixture of groundwater and water purified by reverse osmosis, to reach a  
166 conductivity of  $300 \mu\text{S.cm}^{-1}$ . Each experiment was conducted at  $21^\circ\text{C}$  under a 16:8-h light-  
167 dark photoperiod. The OW was renewed four times per day to maintain adequate water  
168 quality and oxygenation. Ancillary parameters such as pH, dissolved oxygen concentration,

169 conductivity,  $\text{NO}_2^-$ , and  $\text{NH}_4^+$  were monitored.

#### 170 3.2.4. Accumulation test at several exposure concentrations

171 Three aquaria ( $38 \times 20 \times 24.5$  cm in polystyrene) were prepared with 4 L of homogenized  
172 sediment and 15 L of OW: one with field sediment, one with C2-spiked sediment and the last  
173 one with C3-spiked sediment. Three control aquaria were prepared in parallel with silica sand  
174 (particle size distribution: 90% 50–200  $\mu\text{m}$ , 10% <50  $\mu\text{m}$ ). A total of 2400 L4 larvae were  
175 added to sediment and control aquaria (400 in each aquarium). After 4 days of exposure (Fig.  
176 S1– part A), chironomids from both test and control aquaria were collected and  
177 cryopreserved, as explained below in section 3.2.6.

#### 178 3.2.5. Elimination test

179 Four more aquaria were prepared, each with 4 L of homogenized sediment spiked with  
180 PFTTrDA (i.e. C1) with 15 L of OW. One control aquarium was prepared with silica sand  
181 having the same characteristics and origin as in the accumulation test. A total of ca. 4.000 L4  
182 larvae were added to the spiked-sediment aquaria (1000 in each aquarium), and 400 L4 larvae  
183 were added to the control aquarium. After 2 days of exposure, up to 400 larvae were collected  
184 in the sediment; the larvae remaining in the spiked-sediment aquarium were directly (without  
185 gut clearance phase) transferred to three aquaria (400 larvae in each aquarium) containing  
186 silicate sand and clean water for the depuration phase. Similarly, 1.200 remaining larvae from  
187 the field sediment aquaria were directly (without gut clearance phase) transferred to three  
188 aquaria prepared with silica and clean water. The organisms were collected and sacrificed  
189 after 6 h, 18 h, and 42 h of depuration (one aquarium stopped at each time); finally, 42 h after  
190 the transfer the control organisms were also sacrificed (Fig. S1 – part B).

191 The same design was applied to field (un-spiked) sediment.

#### 192 3.2.6. Sample collection and organism measurements

193 The OW was sampled in 1-L polyethylene (PE) bottles and the pore water (PW) was sampled  
194 with a porous polymer micro-sampler (Rhizon® system, SDEC, Reignac-sur-Indre, France;  
195 description in SI). At the end of exposure, subsamples from sediment were deposited in PE  
196 tubes. Chironomids were collected by sieving sediment or silica at 500 µm; about 200 larvae  
197 (ca 800 mg ww or 200 mg dw) were pooled and cryopreserved in liquid nitrogen and then  
198 stored at -21°C before PFAS analysis. As *C. riparius* gut contents represent about 6 % of the  
199 total body weight (Ferrari et al., 2014), and gut clearance was not feasible in the elimination  
200 test, organisms were directly sacrificed. Water and sediment samples were frozen and kept at  
201 -21°C. Additionally, initial body residue was determined by pooling and cryopreserving  
202 about 200 individuals at the start of each experiment.

203 Chironomid survival, length and (wet) weight were determined for each time point, including  
204 the start of each experiment. To determine the total length, four groups of ten larvae were  
205 photographed and the mean sizes determined using digital image analysis software  
206 (Jmicrovision, available free at <http://www.jmicrovision.com/>). The same groups were then  
207 weighed (weighing scales: Sartorius CPA225D, France) to obtain mean individual masses.

### 208 3.3. PFAS analysis

#### 209 3.3.1. PFAS extraction

210 The PFAS extraction methods for OW, PW and sediment samples were similar to those  
211 described in Bertin et al. (2014). Briefly, PFASs were extracted from water samples using  
212 Phenomenex Strata-XAW cartridges while sonication in methanol was used for sediment  
213 samples, followed by graphitized carbon black clean-up. For the chironomid samples, the  
214 method was adapted with minor modifications: both neutral and acid analytes were eluted in a  
215 single fraction using MeOH containing 0.2% NH<sub>4</sub>OH (30% in water). <sup>13</sup>C-labeled PFAS  
216 internal standards (ISs) were added before the extraction. PFASs were analyzed on freeze-  
217 dried tissues based on 800 mg wet weight (ww) for *C. riparius* and 120 mg dry weight for the

218 SRM 1947 fish reference matrix(Reiner et al., 2012).

### 219 3.3.2. LC-MS/MS analysis

220 PFASs were analysed using an Agilent 1200 LC system (Agilent Technologies, Massy,  
221 France) interfaced with an Agilent 6460 triple quadrupole mass spectrometer (details in Table  
222 S3).

### 223 3.3.3. Quality control and methods

224 Analyte recovery was determined using spiked samples ( $n=3$ ) for each matrix (surface and  
225 pore water, sediment, and chironomids) within the range 50-123% (Table S4).

226 Replicate procedural blanks were analysed for each series of samples. PFAS concentrations  
227 were blank-corrected when applicable. For compounds present in blanks, the limits of  
228 detection (LDs) were defined as three times the standard deviation of the blank, and the limits  
229 of quantification (LQs) were set at ten times the standard deviation of the blank. For analytes  
230 not detected in the blanks, LDs ( $0.001\text{--}0.103\text{ ng.g}^{-1}$  or  $\text{ng.L}^{-1}$ ) and LQs ( $0.003\text{--}0.310\text{ ng.g}^{-1}$  or  
231  $\text{ng.L}^{-1}$ ) were determined as the concentration with a signal-to-noise ratio of 3 and 9,  
232 respectively. This was calculated on matrices spiked at  $0.3\text{--}1.1\text{ ng.g}^{-1}$  (sediment and *C.*  
233 *riparius*) and  $0.7\text{--}1.4\text{ ng.L}^{-1}$  (Vittel® mineral water samples) (Table S5). The PFASs  
234 measured in SRM 1947 Lake Michigan Fish Tissue and compared with the NIST value are  
235 presented in SI (Table S6).

### 236 3.4. Data analyses and modelling

237 Data were checked for normality using the Shapiro-Wilk test and were analysed using the  
238 Student *t*-test. Experimental biota-to-sediment accumulation factors ( $BSAF_{exp}$ ) were  
239 determined by dividing tissue concentrations ( $C_{org}$ ,  $\text{ng.g}^{-1}$  ww) at steady state by  
240 concentrations in sediment normalized by  $f_{oc}$  ( $C_{sed-oc} = C_{sed}/f_{oc}$   $\text{ng.g}_{oc}^{-1}$  dw) (Ankley, 1992;  
241 Burkhard et al., 2012). As lipids do not influence PFAS accumulation in tissues, it is not

242 appropriate to adjust  $C_{org}$  to chironomid lipid content (Higgins et al., 2007).

243 Concerning the bioaccumulation modelling, two different hypotheses were tested: (H1)  
244 concentration dependency (Eq. 4), and (H2) no concentration-dependency (Eq. 2). The model  
245 parameter values (depending on the hypothesis) were adjusted simultaneously in order to  
246 obtain the best fit to experimental data. The uptake and elimination coefficient ( $k_u$  and  $k_e$ ), the  
247 half-saturation concentration ( $C_{50}$ ) and the growth rate ( $r$ ) were adjusted simultaneously by  
248 minimizing the weighted least squares between the simulated and observed data. For each  
249 hypothesis, the distance and the adjusted coefficient of determination ( $R^2$ ) were calculated.

250 Model calculations and data analyses were performed with R software (R-Core-team, 2012)  
251 within the RStudio environment (Version 0.97.336).

## 252 4. Results

### 253 4.1. Sediment contamination

254 Long chain perfluoro-alkyl carboxylates were predominant in field sediments: PFUnDA ( $0.85$   
255  $\pm 0.11$  ng.g dw<sup>-1</sup> and  $0.91 \pm 0.26$  ng.g<sup>-1</sup> dw) and PFTrDA ( $1.64 \pm 0.03$  ng.g dw<sup>-1</sup> and  $1.67 \pm$   
256  $0.48$  ng.g<sup>-1</sup> dw) in March and November respectively. PFOS ( $0.58 \pm 0.05$  ng.g dw<sup>-1</sup> and  $0.36 \pm$   
257  $0.13$  ng.g<sup>-1</sup> dw) and FOSA ( $0.03 \pm 0.01$  ng.g dw<sup>-1</sup> and  $0.045 \pm 0.02$  ng.g dw<sup>-1</sup>) were observed  
258 at much lower concentrations. PFTrDA strongly sorbed onto sediment particles and its  
259 concentration increased with the increasing spiking level: after spiking the measured PFTrDA  
260 were  $3.66 \pm 0.48$  ng.g<sup>-1</sup> dw (C1);  $5.83 \pm 0.72$  ng.g<sup>-1</sup> dw (C2);  $10.78 \pm 0.64$  ng.g<sup>-1</sup> dw (C3)  
261 (Fig.S2; Table S7). PFTrDA concentrations apparently decreased during the tests by 43 % in  
262 one instance (C2); they might have decreased slightly in the other instances, by about 10%  
263 (field, C3), to 25 % (field) (Table S6 in SI), so within the range of the analytical uncertainty.

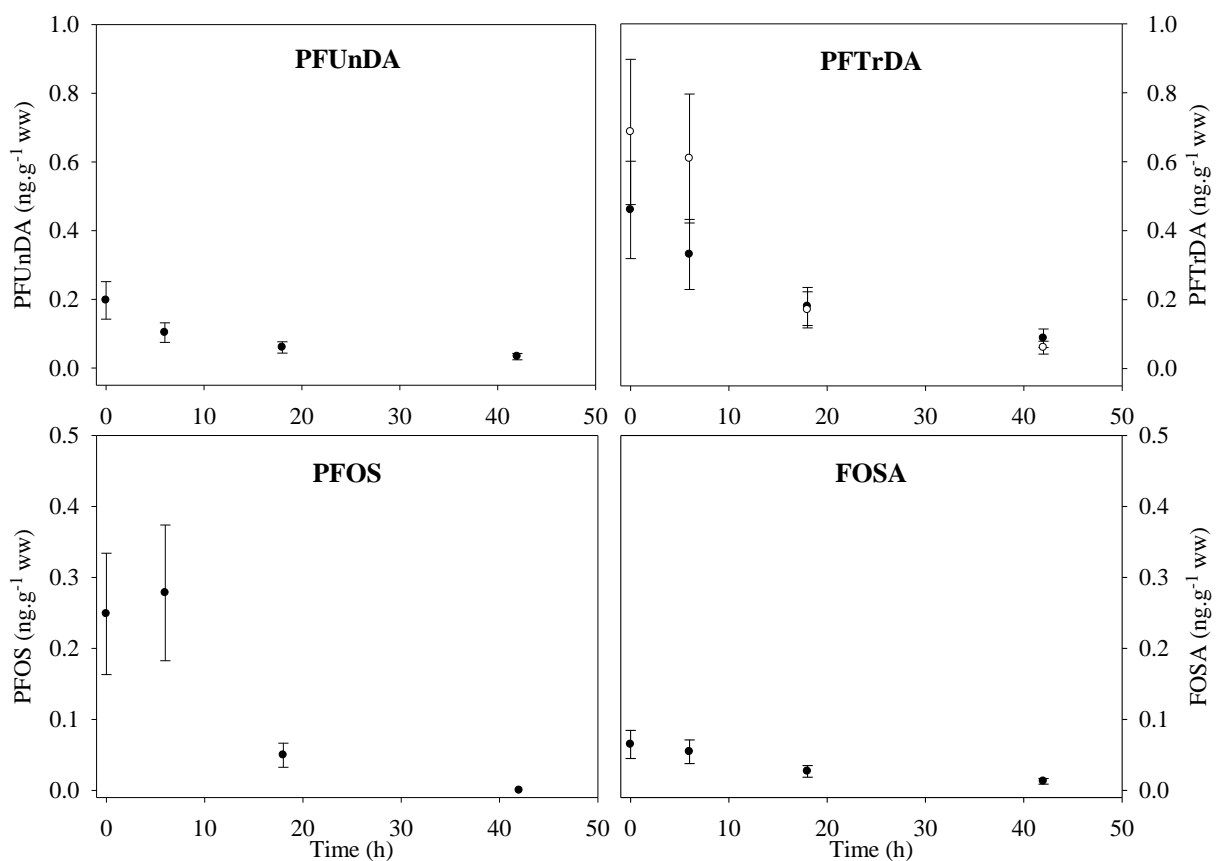
### 264 4.2. Chironomids : survival and PFAS depuration kinetics

265 In the accumulation experiment, chironomid survival at each condition was 97.0%, 92.8% and

266 96.0% for the test samples (field sediment, C2, and C3, respectively) and  $97.1 \pm 2.9\%$  for the  
267 control sample. In the elimination experiment, chironomid survival was  $96.4 \pm 2.6\%$  and  $62.8$   
268  $\pm 17.7\%$  for the test and  $81.9\%$  and  $91.1 \pm 4.0\%$  for the control samples, respectively. The  
269 larva length data fit a linear growth model well ( $R^2 = 0.798$ ).

270 Concentrations in control treatments were systematically below LDs. The chironomids  
271 accumulated two PFCAs (PFUnDA and PFTrDA) as well as PFOS and its precursor FOSA  
272 (Figure 1). For all compounds, PFAS elimination was nearly complete in 42 h.

273 **Figure 1:** Elimination kinetics of PFASs in chironomids exposed to field sediment (unspiked:  
274 black; spiked: open symbols) for each PFAS. Error bars correspond to the analytical  
275 uncertainty.

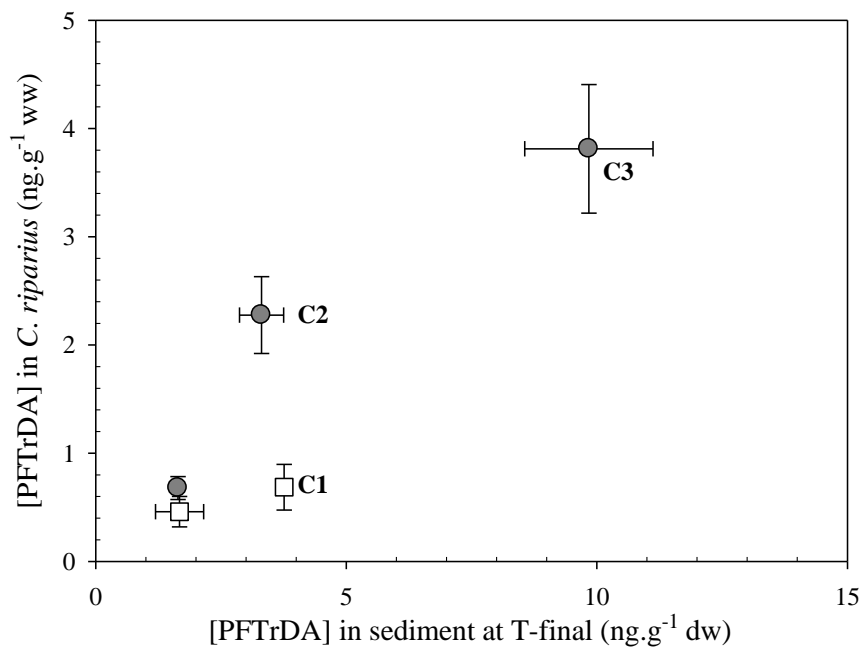


276

277 In all these experiments, the PFTrDA concentration increase in spiked sediments was more  
278 important than in chironomids (Figure 2): while the raw sediment concentration increased by

279 a factor  $\approx 2-3$  in (C2) and  $\approx 6$  (C3), the respective increase rates in chironomids were  $\approx 1.5$   
 280 (C1), 3.4 (C2) and 5.6 (C3). This pattern was more evident when PFTrDA concentrations in  
 281 sediment were adjusted to organic carbon content (Table 1).

282 **Figure 2:** Biplot of PFTrDA concentrations in sediment (X-axis) and *C. riparius* (Y-axis);  
 283 error bars account for the analytical uncertainty; open squares: November field sediment and  
 284 related spiked sediment (C1); gray dots: March field sediment and related spiked sediments  
 285 (C2, C3).



286  
 287 Nevertheless, the  $BSAF_{exp}$  resulting from the different exposure conditions (Table 1) did not  
 288 differ much, unlike what should have occurred in case of concentration dependency, where  
 289 the BSAF should decrease while the  $f_{oc}$  adjusted PFTrDA sediment concentrations increase.  
 290 Nevertheless the  $BSAF_{exp}$  resulting from the C1 experiment was obtained after a reduced  
 291 exposure time, and might thus be underestimated.

Experiments	Type	Sediment organic matter (ng <sub>oc</sub> .g <sup>-1</sup> dw)	Chironomids (ng.g <sup>-1</sup> ww)	$BSAF_{exp}$
Accumulation phase of the	Field	65.92 ± 1.79	0.460 ± 0.141	0.007 ± 0.0039

elimination test	C1	168.61 ± 4.04	0.686 ± 0.211	0.004 ± 0.0023
Accumulation test	Field	57.67 ± 7.44	0.678 ± 0.106	0.012 ± 0.0007
	C2	153.95 ± 20.47	2.276 ± 0.355	0.015 ± 0.0007
	C3	457.67 ± 59.53	3.812 ± 0.594	0.008 ± 0.0004

292 **Table 1** – PFTrDA concentrations in sediment organic matter and chironomids at  $T_{\text{final}}$  and  
 293 resulting  $BSAF_{\text{exp}}$

294  $BSAF_{\text{exp}}$  calculated for PFUnDA, PFOS and FOSA are recorded in SI, Table S8; they are in  
 295 the same range as for PFTrDA, between 0.006 – 0.007 for PFUnDA and 0.013 – 0.022 for  
 296 FOSA.

### 297 4.3. Model outcomes

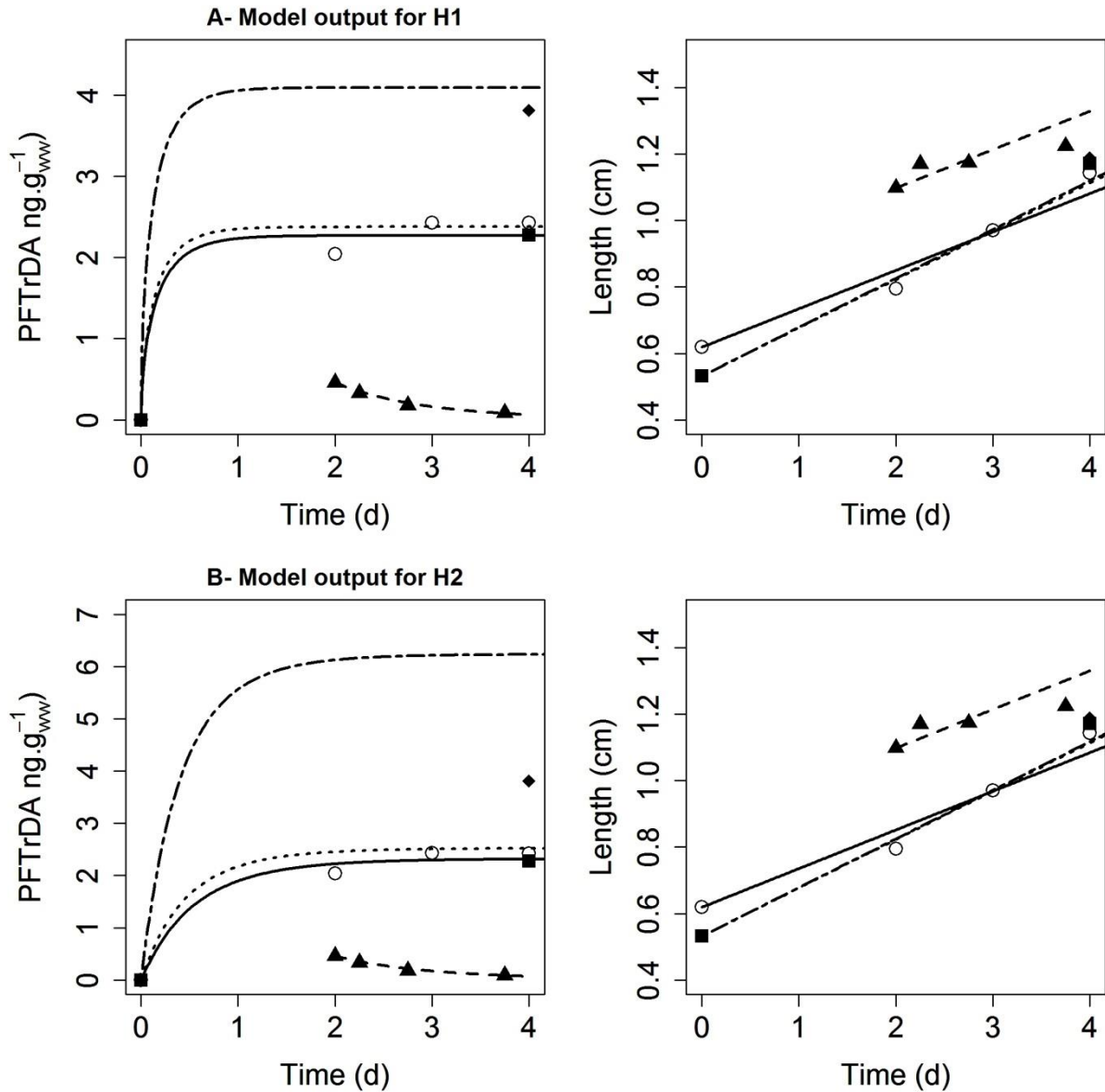
298 The model parameters ( $k_u$ ,  $k_e$ ,  $r$  and  $C_{50}$  for PFTrDA in the case of H1;  $k_u$ ,  $k_e$  and  $r$  for  
 299 PFTrDA in the case of H2) were adjusted simultaneously on the basis of all results in order to  
 300 obtain the best fit to the data by minimizing the weighed least squares between simulated and  
 301 observed data.

302 The final uptake and elimination rates for PFTrDA are presented in Table 2. There was much  
 303 better agreement between observed and simulated data for H1 (adjusted  $R^2$  0.978, distance  
 304 1.279; Figure 3-A) than for H2 (adjusted  $R^2$  0.655, distance 13.919; Figure 3-B).

Hypotheses	$k_u$ ( $\text{g}_{\text{oc}} \cdot \text{g}_{\text{ww}} \cdot \text{h}^{-1}$ )	$k_e$ ( $\text{h}^{-1}$ )
H1	0.013 ± 0.008	0.032 ± 0.009
H2	0.00077 ± 7.5*10 <sup>-5</sup>	0.0098 ± 0.0042

305 **Table 2** - Optimized uptake and depuration constants for PFTrDA.

306 Growth curves displayed in Figure 3-A and B (right-hand panels, fitted simultaneously with  
 307 accumulation data) are essentially identical, as they rely on the same data. Slopes (growth  
 308 rates) did not differ between the experiments, and between field and spiked sediments.



309

310 **Figure 3** - Observed (symbols) and simulated (lines) PFTrDA concentrations (left hand  
311 panels, ng.g<sup>-1</sup> ww) and chironomid growth (right hand panels, mm) for H1 (A) or H2 (B)  
312 models (square/solid line: field; open dots/dotted line: C2; diamonds/sash-dot line: C3;  
313 triangle/dash line: depuration phase).

314 PFTrDA half-life ( $T_{1/2}$ ) on the basis of model H1 was 0.65 day. .

## 315 5. Discussion

### 316 5.1. Sediment spiking

317 The sediment contamination profile at the sampling site is rather unusual, with PFTrDA

318 contributing up to 36 % to the sum of PFAS concentrations (Munoz et al., 2015), and  
319 reaching concentrations as high as  $1.67 \pm 0.48 \text{ ng.g}^{-1} \text{ dw}$ , which is comparable to Zushi et al.  
320 (2010). These authors measured this compound at  $1.2 \text{ ng.g}^{-1}(\text{dw})$  in Tokyo Bay sediment.  
321 Only a few other studies looked for this chemical (e.g. Zhao et al., 2015), and generally found  
322 lower concentrations than in this study. While it is therefore very difficult to confirm whether  
323 or not the spiking schedule was realistic, we considered that this was not a significant  
324 concern, given that the motivation for spiking was to determine whether or not concentration  
325 dependency occurs.

## 326 5.2. Uptake and elimination kinetics

327 The comparison of model performances for the two hypotheses shows a much better fit to  
328 experimental data for H1. The discussion about uptake and elimination kinetics is accordingly  
329 focused on H1 model outcomes. PFTrDA elimination by chironomids is quick even when  
330 adjusting for growth; indeed, the elimination constant equaled  $0.032 (\pm 0.009) \text{ h}^{-1}$  when  
331 calculated under the H1 hypothesis, with simultaneous optimization of both  $k_u$  and  $k_e$  (Table  
332 2). This  $k_e$  value is very similar to the  $k_e$  value determined in our previous study (Bertin et al.,  
333 2014) using a partition model with a correction for growth, i.e.  $0.03 \pm 0.01 \text{ h}^{-1}$ . Conversely,  
334 the  $k_u$  value derived under the H1 hypothesis is about one order of magnitude greater than the  
335  $k_u$  derived previously ( $0.0015 \text{ g}_{\text{oc}}\cdot\text{g}_{\text{ww}}\cdot\text{h}^{-1}$ ; Bertin et al., 2014), emphasizing the impact of  
336 model choice. However, in the present study, the proposed model takes into account the  
337 growth dilution for both uptake and elimination phases, with the length of the organisms  
338 introduced in each term of the model equation (Eq. 4). In addition,  $k_u$  and  $k_e$  were estimated  
339 from the same experimental data set, and estimated together. The  $k_u$  and  $k_e$  obtained in the  
340 present study under the concentration-dependency hypothesis are therefore more reliable than  
341 those calculated under a passive diffusion hypothesis on the basis of the accumulation phase  
342 only, or separately for two phases. Meanwhile, the BSAF values of ( $BSAF_{\text{exp}}$ , Table 1) did not

343 support the concentration-dependency hypothesis. The steady state might not be reached after  
344 2 days of exposure, and the growth dilution is not taken into account for the  $BSAF_{exp}$   
345 calculation, which may explain why BSAFs did not follow the expected pattern.

346 Our experimental results did not allow for testing the concentration-dependency hypothesis  
347 for other PPFASs, such as PFUnDA or PFOS, nor to derive kinetic BSAFs by solving  
348 analytically Eq. 2, due to the growth dilution term. Overall, these BSAFs were low,  
349 confirming some field evidence (Babut et al., 2017) that chironomids would not be a  
350 significant source of PFTrDA and other PFCAs to their predators, e.g. fish.

## 351 **6. Conclusion**

352 The models tested herein are advantageous in that they simultaneously optimize the uptake  
353 and elimination rates while accounting for chironomid growth rate, in contrast to other studies  
354 that calculated the uptake and elimination rates from two different models (Higgins et al.,  
355 2007; Higgins et al., 2009; Van Geest et al., 2011).

356 Reliable experimental elimination constants ( $k_e$ ) were obtained for chironomids exposed to a  
357 field sediment contaminated by a PFAS mixture (PFTrDA, PFUnDA, and to a lesser extent  
358 PFOS, FOSA). Measured PFTrDA concentrations accumulated in chironomid tissues did not  
359 increase proportionally to their increase in sediment, but the resulting experimental BSAFs  
360 did not vary much. Nevertheless, bioaccumulation modeling with a simultaneous optimization  
361 of uptake and elimination rates consistently supported the hypothesis of concentration-  
362 dependency for this compound and yielded reliable uptake and elimination rates. Similar  
363 findings were reported by for shorter chain PFCAs (PFOA, PFNA, PFDA) in the green  
364 mussel (*Perna viridis*) (Liu et al., 2011), suggesting that concentration dependency could be a  
365 rather general uptake mechanism for long chain PFCAs or PFSAs.

366

367 **Acknowledgements**

368 This study was supported by the Rhone-Mediterranean and Corsica Water Agency and the  
369 Rhone-Alpes Region within the Rhone ecological restoration plan. The Aquitaine Region and  
370 the European Union [CPER A2E project] are acknowledged for their financial support. This  
371 study also benefitted from grants of the French National Research Agency (ANR) as part of  
372 the Investments for the future Program, within the Cluster of Excellence COTE [ANR-10-  
373 LABX-45]. We thank Linda Northrup (English Solutions, Voiron, France) for copyediting the  
374 text.

375

376 **References**

- 377 Ahrens, L., et al., 2009. Partitioning Behavior of Per- and Polyfluoroalkyl Compounds between Pore  
378 Water and Sediment in Two Sediment Cores from Tokyo Bay, Japan. *Environmental Science  
379 & Technology*. 43, 6969-6975.
- 380 Ankley, G. T., 1992. Bioaccumulation of PCBs from sediments by oligochaetes and fishes: comparison  
381 of laboratory and field studies. *Canadian Journal of Fisheries & Aquatic Sciences*. 49, 2080-  
382 2085.
- 383 Babut, M., et al., 2017. Per- and poly-fluoroalkyl compounds in freshwater fish from the Rhône River:  
384 influence of fish size, diet, prey contamination and biotransformation. *Science of the Total  
385 Environment*. 605-606, 38-47.
- 386 Bao, J., et al., 2009. Perfluorinated compounds in sediments from the Daliao River system of  
387 northeast China. *Chemosphere*. 77, 652-657.
- 388 Bao, J., et al., 2010. Perfluorinated compounds in urban river sediments from Guangzhou and  
389 Shanghai of China. *Chemosphere*. 80, 123-130.
- 390 Bertin, D., et al., 2014. Bioaccumulation of perfluoroalkyl compounds in midge (*Chironomus riparius*)  
391 larvae exposed to sediment. *Environmental Pollution*. 189, 27-34.
- 392 Bertin, D., et al., 2016. Potential exposure routes and accumulation kinetics for poly- and  
393 perfluorinated alkyl compounds for a freshwater amphipod: *Gammarus* spp. (Crustacea).  
394 *Chemosphere*. 155, 380-387.
- 395 Bhhatarai, B., Gramatica, P., 2011. Prediction of Aqueous Solubility, Vapor Pressure and Critical  
396 Micelle Concentration for Aquatic Partitioning of Perfluorinated Chemicals. *Environmental  
397 Science & Technology*. 45, 8120-8128.
- 398 Burkhard, L. P., et al., 2012. Comparing laboratory- and field-measured biota-sediment accumulation  
399 factors. *Integrated Environmental Assessment and Management*. 8, 32-41.
- 400 Dauchy, X., et al., 2012. Relationship Between Industrial Discharges and Contamination of Raw Water  
401 Resources by Perfluorinated Compounds. Part I: Case Study of a Fluoropolymer  
402 Manufacturing Plant. *Bulletin of Environmental Contamination and Toxicology*. 89, 525-530.
- 403 Ferrari, B. J. D., et al., 2014. Bioaccumulation kinetics and effects of sediment-bound contaminants  
404 on chironomids in deep waters: New insights using a low-disturbance in situ system.  
405 *Environmental Technology (United Kingdom)*. 35, 456-469.
- 406 Greaves, A. K., et al., 2013. Brain region distribution and patterns of bioaccumulative perfluoroalkyl  
407 carboxylates and sulfonates in east greenland polar bears (*Ursus maritimus*). *Environmental*

- 408 Toxicology and Chemistry. 32, 713-722.
- 409 Higgins, C. P., et al., 2005. Quantitative determination of perfluorochemicals in sediments and  
410 domestic sludge. *Environmental Science and Technology*. 39, 3946-3956.
- 411 Higgins, C. P., et al., 2007. Bioaccumulation of perfluorochemicals in sediments by the aquatic  
412 oligochaete *Lumbriculus variegatus*. *Environmental Science and Technology*. 41, 4600-4606.
- 413 Higgins, C. P., et al., 2009. Bioaccumulation of triclocarban in *Lumbriculus variegatus*. *Environmental*  
414 *Toxicology and Chemistry*. 28, 2580-2586.
- 415 Houde, M., et al., 2011. Monitoring of Perfluorinated Compounds in Aquatic Biota: An Updated  
416 Review. *Environmental Science & Technology*. 45, 7962-7973.
- 417 Houde, M., et al., 2006. Biological monitoring of polyfluoroalkyl substances: A review. *Environmental*  
418 *Science and Technology*. 40, 3463-3473.
- 419 Labadie, P., Chevreuil, M., 2011. Partitioning behaviour of perfluorinated alkyl contaminants  
420 between water, sediment and fish in the Orge River (nearby Paris, France). *Environmental*  
421 *Pollution*. 159, 391-397.
- 422 Lasier, P. J., et al., 2011. Perfluorinated chemicals in surface waters and sediments from northwest  
423 Georgia, USA, and their bioaccumulation in *Lumbriculus variegatus*. *Environmental*  
424 *Toxicology and Chemistry*. 30, 2194-2201.
- 425 Liu, C., et al., 2011. Novel Perspectives on the Bioaccumulation of PFCs – the Concentration  
426 Dependency. *Environmental Science & Technology*. 45, 9758-9764.
- 427 Martin, J. W., et al., 2004. Perfluoroalkyl contaminants in a food web from lake Ontario.  
428 *Environmental Science & Technology*. 38, 5379-5385.
- 429 Munoz, G., et al., 2015. Spatial distribution and partitioning behavior of selected poly- and  
430 perfluoroalkyl substances in freshwater ecosystems: A French nationwide survey. *Science of*  
431 *The Total Environment*. 517, 48-56.
- 432 Myers, A. L., et al., 2012. Fate, distribution, and contrasting temporal trends of perfluoroalkyl  
433 substances (PFASs) in Lake Ontario, Canada. *Environment International*. 44, 92-99.
- 434 Péry, A. R. R., et al., 2002. A modeling approach to link food availability, growth, emergence, and  
435 reproduction for the midge *Chironomus riparius*. *Environmental Toxicology and Chemistry*.  
436 21, 2507-2513.
- 437 Prevedouros, K., et al., 2006. Sources, fate and transport of perfluorocarboxylates. *Environmental*  
438 *Science and Technology*. 40, 32-44.
- 439 Prosser, R. S., et al., 2016. Bioaccumulation of perfluorinated carboxylates and sulfonates and  
440 polychlorinated biphenyls in laboratory-cultured *Hexagenia* spp., *Lumbriculus variegatus* and  
441 *Pimephales promelas* from field-collected sediments. *Science of the Total Environment*. 543,  
442 715-726.
- 443 R-Core-team, R: A language and environment for statistical computing. R Foundation for Statistical  
444 Computing. In: R. F. f. S. Computing, (Ed.), Vienna (Austria), 2012.
- 445 Reiner, J. L., et al., 2012. Determination of perfluorinated alkyl acid concentrations in biological  
446 standard reference materials. *Analytical and Bioanalytical Chemistry*. 1-10.
- 447 Van Geest, J. L., et al., 2011. Accumulation and Depuration of Polychlorinated Biphenyls from Field-  
448 Collected Sediment in Three Freshwater Organisms. *Environmental Science & Technology*.  
449 45, 7011-7018.
- 450 Zhao, Z., et al., 2015. Spatial distribution of perfluoroalkyl acids in surface sediments of the German  
451 Bight, North Sea. *Science of the Total Environment*. 511, 145-152.
- 452 Zushi, Y., et al., 2010. Time trends of perfluorinated compounds from the sediment core of Tokyo  
453 Bay, Japan (1950s-2004). *Environmental Pollution*. 158, 756-763.

454

455